Organic & Biomolecular Chemistry

This article is part of the

OBC 10th anniversary

themed issue

All articles in this issue will be gathered together online at

www.rsc.org/OBC10

Organic & Biomolecular Chemistry

Dynamic Article Links
View Online

Cite this: *Org. Biomol. Chem.*, 2012, **10**, 5845

www.rsc.org/obc

PAPER

Solvent and substituent effects on aggregation constants of perylene bisimide π-stacks – a linear free energy relationship analysis†

Zhijian Chen,[a,b] Benjamin Fimmel[a] and Frank Würthner*[a]

Received 19th December 2011, Accepted 30th January 2012
DOI: 10.1039/c2ob07131b

A series of six perylene bisimides (PBIs) with hydrophilic and hydrophobic side chains at the imide nitrogens were applied for a comparative study of the solvent and structural effects on the aggregation behaviour of this class of dyes. A comparison of the binding constants in tetrachloromethane at room temperature revealed the highest binding constant of about 10^5 M^{-1} for a PBI bearing 3,4,5-tridodecyloxyphenyl substituents at the imide nitrogens, followed by 3,4,5-tridodecylphenyl and alkyl-substituted PBIs, whereas no aggregation could be observed in the accessible concentration range for PBIs equipped with bulky 2,6-diisopropylphenyl substituents at the imide nitrogens. The aggregation behaviour of three properly soluble compounds was investigated in 17 different solvents covering a broad polarity range from nonpolar *n*-hexane to highly polar DMSO and water. Linear free energy relationships (LFER) revealed a biphasic behaviour between Gibbs free energies of aggregation and common empirical solvent polarity scales indicating particularly strong π–π stacking interactions in nonpolar aliphatic and polar alcoholic solvents whilst the weakest binding is observed in dichloromethane and chloroform. Accordingly, PBI aggregation is dominated by electrostatic interactions in nonpolar solvents and by solvophobic interactions in protic solvents. In water, the aggregation constant is increased far beyond LFER expectations pointing at a pronounced hydrophobic effect.

Introduction

Being one of the most important noncovalent interactions for self-assembly, π–π stacking of aromatic molecules has attracted considerable attention in the past decades.[1] In nature, this interaction is ubiquitous and provides important contribution for the structural stabilization of biomacromolecules such as DNA and proteins.[2] Furthermore, π–π interactions play a key role in the formation of rod-like or cyclic aggregates of chlorophyll chromophores which act as the central units in the light harvesting complexes of plants and bacteria.[3] In artificial systems, the stacking of π-conjugated molecules leads to the formation of J- or H-type aggregates,[4] organogels[5] or columnar liquid crystals,[6] which have been applied as advanced functional materials in the fields of organic electronics,[7] solar energy conversion[8] or biosensors.[9]

Owing to its complexity, the nature of the π–π interaction has been debated for a long time.[10,11] Previous studies have also revealed that the π–π stacking of aromatic molecules is strongly influenced by the solvent.[1,12–17] In 1990, Smithrud and Diederich have investigated in their seminal study the encapsulation of a pyrene guest in a macrocyclic cyclophane host in 17 different organic solvents and water.[12] The important outcome of this study was a linear free energy relationship (LFER)[13] between the Gibbs free binding energy and the empirical solvent parameter $E_T(30)$. The regression analysis showed that the most stable complexes between these apolar molecules formed in polar solvents. Accordingly, the largest Gibbs free binding energy was measured in water, but quite remarkably, without a significant deviation from the regression line as might have been expected owing to the hydrophobic effect. It is noteworthy, however, that aliphatic solvents were not included in this study, presumably owing to the lack of solubility of the macrocyclic host in such solvents. In the following years solvent-dependent aggregation has been applied by many groups to direct the self-assembly or the folding of π-conjugated molecules[14] or to achieve nano- and microcrystalline materials, in particular by the reprecipitation approach.[15] A detailed examination of the different contributions to the Gibbs free energy of π–π stacking, such as electrostatic and dispersion interactions as well as charge-transfer and hydrophobic interactions has, however, been rarely pursued in these studies. An exception is the investigation of Cubberley and Iverson who studied the solvent effects on the donor–donor,

[a]*Universität Würzburg, Institut für Organische Chemie and Center for Nanosystems Chemistry, Am Hubland, 97074 Würzburg, Germany. E-mail: wuerthner@chemie.uni-wuerzburg.de; Fax: +49 931 31 84756*
[b]*School of Chemical Engineering and Technology, Tianjin University, Tianjin, 300072, China*

† This article is part of the *Organic & Biomolecular Chemistry* 10th Anniversary issue

acceptor–acceptor, and donor–acceptor aromatic stacking for a 1,5-dialkoxynaphthalene donor and a naphthalene tetracarboxylic bisimide acceptor in nine solvents ranging from chloroform as lowest polarity solvent to water as the most polar solvent.[16] The results showed that the solvophobic effect as well as the electrostatic interaction of the donor and acceptor molecules played important roles in the aromatic stacking of these molecules. Remarkably, again a quite reasonable correlation for the Gibbs free binding energy for the 1 : 1 donor–acceptor complex was observed with the empirical solvent polarity parameter $E_T(30)$. In addition, like for the Diederichs cyclophane–pyrene complex the strongest binding was observed in the most polar solvents which is against the common intuition with regard to charge transfer or electrostatic interactions. In another study our group elucidated the solvent effect on the dimerization of dipolar merocyanine dyes for eight solvents situated more on the lower polarity side, *i.e.* from tetrachloromethane to dichloroethane.[17] Here, the results showed that the binding strength was reduced upon increasing polarity pointing at a dominant electrostatic contribution to the thermodynamic stabilization of those aggregates formed from highly dipolar dyes.

Another factor that plays an important role in the π–π stacking is the effect of peripheral substituents attached at the aromatic core of the molecules. Moore and coworkers reported that the aggregation behaviour is significantly different for the hexakis (phenylene ethynylene) macrocycles with various side chains and linking groups.[18] In another example,[19] Müllen and coworkers reported the influence of different kinds of alkyl substituents on the π–π stacking of hexabenzocoronenes in solution as well as on surfaces. In our studies, substituent effects on the dimerization of merocyanine dyes were also observed.[17b]

Within the class of functional π-conjugated molecules, perylene bisimide (PBI) dyes were investigated most extensively due to their strong photoluminescence and excellent n-type semiconductor properties.[8a,20] Owing to the strong intermolecular interactions between these quadrupolar dyes,[1c] well ordered columnar π-stacks in solution and in liquid-crystalline mesophases have been observed for a variety of PBI derivatives that are only distinguished by the respective solubilizing chains at the imide positions.[21] The pronounced similarity in the optical and charge transport properties of these PBI dye aggregates corroborate a preferential stacking arrangement between the dyes with rotational offsets of about 30°, a value that has been deduced as the energy minimum configuration by quantum chemical calculations.[22] A comprehensive study on the effect of different imide substituents and the solvent on the thermodynamics of PBI dye aggregation is, however, still absent despite its importance for the control of interaction strength and aggregate size, *e.g.* for solution processing techniques such as spin-coating in device fabrication for organic electronics.‡

Accordingly, in this paper we will elucidate the influence of the solvent and different solubilizing side chains at imide substituents on the π–π stacking forces between PBI molecules. The investigated PBI derivatives are shown in Fig. 1 and were obtained according to literature procedures[21,23,24] by imidization reactions between the respective amines and perylene–tetracarboxylic acid bisanhydride. The choice of substituents with different hydrophilicity–hydrophobicity afforded PBI dyes whose sufficient solubility for aggregation studies covers a broad polarity range from *n*-hexane to water. Accordingly, this study will shed more light on the nature of π–π interactions of this type of functional dyes and for extended quadrupolar aromatic π-systems in general.

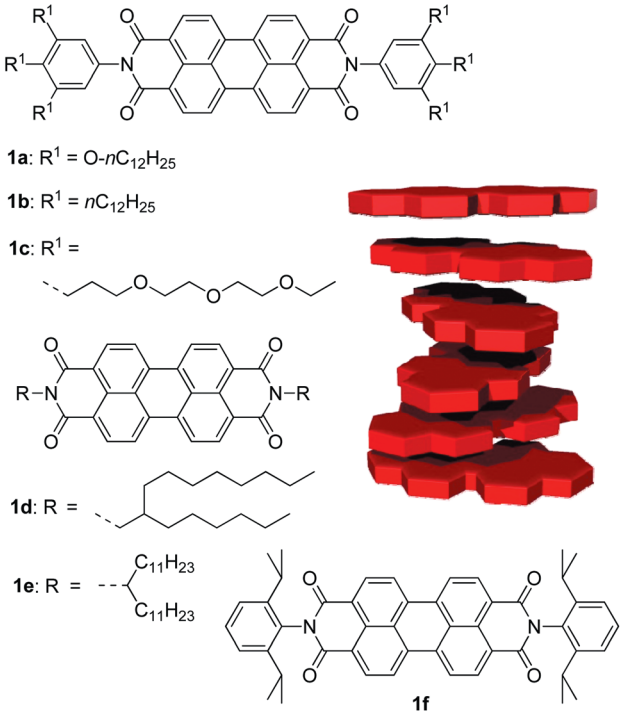

Fig. 1 Chemical structures of the PBI dyes **1a–f** used in this study and sketch for the assumed arrangement of **1a–e** in a columnar aggregate according to experimental and quantum chemical investigations.[21e,22]

Table 1 Peak positions of UV/Vis absorption maxima λ_{abs} and fluorescence maxima λ_{em}, absorption coefficients ε_{max} and fluorescence quantum yields Φ_{em} for PBIs in dichloromethane (**1a–c**) or chloroform (**1d–f**) at 25 °C

PBI	λ_{abs}/nm	ε_{max}/M^{-1} cm^{-1}	λ_{em}/nm	Φ_{em}
1a[a]	527 (529)[d]	89 600	—	0
1b[b]	527	96 300	532	0.63
1c[c]	527	96 400	532	0.68
1d	523	85 600	530	0.99
1e	523	86 100	530	0.99
1f	524	85 000[e]	530	1.00[e]

[a] Data from ref. 21*a*. [b] Data from ref. 21*d*. [c] Data from ref. 21*f*. [d] Value determined in $CHCl_3$. [e] Data from ref. 23.

Results and discussion

UV/Vis absorption and fluorescence spectra of monomeric PBIs

The UV/Vis and fluorescence data of compounds **1a–f** have been reported before and the results are collected for comparison in Table 1. Despite different substituents at the imide nitrogen, the shape and position of the absorption and emission bands of these dyes are almost identical in their non-aggregated state. Each of these compounds display an absorption band between 400 nm and 550 nm (Fig. 2) which can be assigned as the S_0–S_1

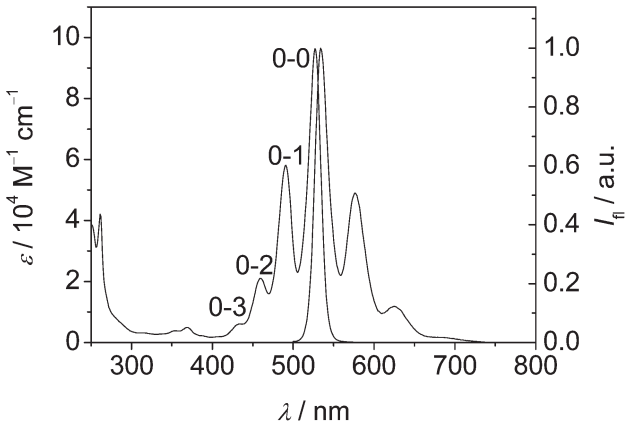

Fig. 2 UV/Vis absorption and fluorescence spectra of PBI **1c** in dichloromethane. The excitation wavelength for the fluorescence spectrum was 480 nm.

electronic transition of the PBI chromophore. The transition dipole moment is polarized along the long axis of the PBI chromophore and strongly coupled with breathing vibration of the perylene skeleton.[24] Thus, well-resolved vibronic structures (0–0, 0–1, 0–2, and 0–3 transitions) can be observed in the S_0–S_1 band with an energy progression of about 1400 cm^{-1}. The compounds **1b–f** are strongly fluorescent and the fluorescence spectra are mirror images of the corresponding absorption bands accompanied by well-resolved fine structures. The fluorescence quantum yields of PBIs **1b,c** in CH_2Cl_2 are 0.63 and 0.68, respectively, whereas no fluorescence can be detected for **1a** which has been attributed to photoinduced electron transfer from the electron-rich trialkylphenoxy substituents to the electron-poor PBI core.[21a,25] Notably, the values for dyes **1b,c** are lower than those of *N*-diisopropyl and *N*-alkyl-substituted PBIs **1d–f** (Φ_{em} > 0.95), indicating that the trialkylphenyl groups (**1b**) already cause a certain degree of fluorescence quenching. In general, the maxima and vibronic progressions of the absorption (Table 1) and the fluorescence spectra are only weakly influenced by the solvent for the monomeric dyes. Accordingly, the solvatochromism is weak in agreement with the lack of a dipole moment in these molecules.[26]

Aggregation in tetrachloromethane

For a comparison of the aggregation behaviour of the various PBI dyes tetrachloromethane (CCl_4) proved to be the ideal solvent. In this solvent all dyes exhibit reasonable to very high solubility (Table 2) which allowed to study the equilibrium between monomeric and aggregated species over a sufficient concentration range by UV/Vis spectroscopy. However, with the exception of dye **1a** rather high concentrations were required to accomplish a substantial degree of aggregation. Owing to the high concentrations and concomitantly strong absorbance, data analysis was not always possible at the absorption maxima due to the limitation of instrumental resolution and the aggregation process had to be analysed at the rims of the absorption band at λ > 540 nm. In Table 2 we have collected the roughly estimated solubility data and the aggregation constants determined

Table 2 Solubilities, aggregation constants *K*, and corresponding Gibbs free energy changes $\Delta G°$ of PBI dyes **1a–f** in tetrachloromethane at 25 °C

PBI	Solubility/g L^{-1}	K/M^{-1}	$-\Delta G°$/kJ mol^{-1}
1a	>150[a]	1.8×10^5	30.0
1b	>50[a]	650	16.0
1c	>100[a]	1400	17.9
1d	13	220	13.4
1e	[b]	23	7.8
1f	0.25	<2[c]	<1.7[c]

[a] Rough estimation. [b] A very large amount of this dye could be dissolved in only tiny volume of solvent, thus reliable estimation is not possible. [c] No evidence for aggregation up to the solubility limit.

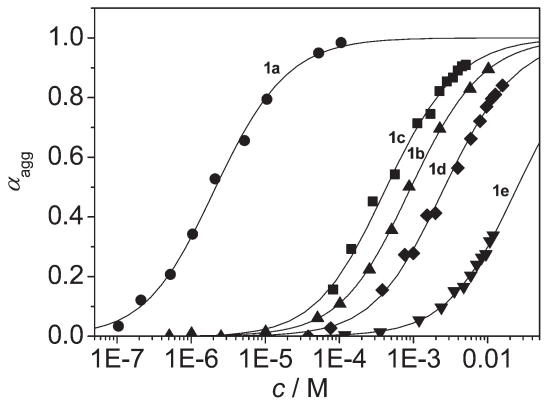

Fig. 3 Molar fraction of aggregated molecules α_{agg} as a function of concentration of the PBI dyes **1a–e** in tetrachloromethane. The lines were obtained by fitting the concentration-dependent UV/Vis data with the isodesmic model.

according to the isodesmic model. Notably, this model assumes equal binding strengths for both PBI π-faces which was unequivocally proven for PBI **1b** in our earlier study.[21e] For the present series of dyes the *K* values were obtained by fitting of the UV/Vis spectral data according to the isodesmic (equal *K*) model[1c,27] with nonlinear least-square regression analysis for at least three different wavelengths. For PBIs **1a–d** we were able to acquire data over a large concentration range that covered the transition from monomeric (degree of aggregation α_{agg} close to zero) to aggregated species (degree of aggregation α_{agg} close to one).

Fig. 3 shows the concentration-dependent transitions from monomeric to aggregated PBI dyes (symbols) and the calculated regression lines according to the isodesmic model. According to this graphical representation as well as from the aggregation constants and Gibbs free energy changes in Table 2 we can draw the conclusion that the "intrinsic" binding constant between PBI dyes is in the range of 10^2–10^3 M^{-1} in CCl_4 as observed for derivatives **1b–d** that bear either aromatic or aliphatic imide substituents without significant steric demand. A substantial increase is observed for PBI **1a** which might be attributed to charge transfer interactions between the electron poor PBI imide units and the electron rich 3,4,5-trialkoxyphenyl units of neighbouring dyes in the π-stack (compare structural model in Fig. 1). On the other hand, no aggregation at all could be observed for PBI **1f** which remains dissolved as a monomeric dye up to rather high

concentrations owing to the very effective sterical shielding by four isopropyl substituents that are located above and below the PBI π-plane. Interestingly, to some extent this effect is also observed for swallow-tail substituted PBI **1e**. As shown by Langhals and coworkers[24] and by Wescott and Mattern,[28] secondary alkyl substituents exhibit restricted rotations around the C–N bond leading to asymmetrical conformation with quite complex NMR signal patterns. For this reason as well as the reduced aggregation constants swallow-tail substituents are less suitable for columnar self-assembly in solution than trialkoxyphenyl and trialkylphenyl substituents.

Solvent-dependent aggregation

To investigate the aggregation behaviour of these compounds, concentration-dependent UV/Vis absorption spectroscopic studies were performed in 17 different solvents including the nonpolar solvent *n*-hexane and the most polar solvent water. Fig. 4 shows representative concentration-dependent UV/Vis spectra recorded in different organic solvents and water for the compounds **1a–c**. In all organic solvents applied here, absorption spectra of molecularly dissolved PBIs were observed at low concentrations. Upon increasing the concentration of the PBI dyes, pronounced spectral changes were observed, providing clear evidence for the aggregation of these PBIs and indicating strong electronic interactions between the aggregated chromophores. In all solvents, upon aggregation a broadening of the absorption band with concomitant decrease of the absorption coefficients is observed. In accordance with exciton coupling theory for a dye stack with rotational displacements of ~30° between the neighbouring dyes,[22] we can assign the major hypsochromically shifted band as H-band and the bathochromically shifted band as J-band.

Fig. 4a and b display the concentration-dependent spectra for the dyes **1a** and **1b** in toluene, respectively. The spectral changes of these two compounds are quite similar but a slight difference can be observed around 470 nm, where the aggregate band of **1a** has a higher ε value. Furthermore, the wavelengths of the absorption maxima of the monomer (λ_{mon}) and aggregate bands (λ_{agg}) of dyes **1a–c** in different solvents are summarized in Table 3. For the dyes **1a–c**, in the same solvent basically identical values of λ_{mon} as well as λ_{agg} are observed. With increasing the polarity of the solvents, the absorption maxima λ_{mon} are bathochromically shifted from 515 nm (**1b** in *n*-hexane) to 533 nm (**1c** in DMSO) while only slight changes of λ_{agg} (491–495 nm) could be observed nearly for all solvents except the most polar DMSO and water. Accordingly, the apparent solvent-dependent spectral changes observed in Fig. 4 result primarily from the solvatochromic shift of the monomer spectra. The spectral properties of the aggregates are little influenced by the environment as long as the media does not change the arrangement of the dyes on top of each other. Thus, for aliphatic solvents (Fig. 4c) a new broad band can be observed at longer wavelength around 540 nm and become stronger upon aggregation while in the more polar solvents like MeOH this band is less obvious because its maximum is close to the one for the monomer.

In water, the aggregation behaviour is significantly different from that in organic solvents. The dye **1c** is water-soluble although the dissolution process is quite slow. When it was mixed with water, the substance started to swell gradually, but no immediate dissolution can be observed like in organic solvents. For the preparation of an aqueous solution of a concentration of 10^{-4} M, at least two days were needed to dissolve all the dye. After this time, however, the aqueous solution remained stable over several months. The UV/Vis spectrum of **1c** in water (Fig. 4f) displays even at low concentrations of $<10^{-5}$ M a broad, structureless absorption band between 400 and 520 nm with an absorption maximum at 485 nm and a second absorption band at longer wavelength with a peak at 550 nm,[21f] which is 10 nm bathochromically shifted compared to the value in methylcyclohexane (MCH). This spectrum indicates that the dye molecules in water are highly aggregated. Upon increasing the temperature, dye **1c** agglomerates and precipitates which is contrary to the monomerization of the PBIs in organic solvents. Similarly, in water an enhanced aggregation at higher temperature has been reported for PBI–DNA conjugates by Wang *et al.*[29] These results indicate that in water the hydrophobic effect plays a key role for the aggregation of PBIs.

From our concentration-dependent UV/Vis data sets for compounds **1a–c** in various solvents at 25 °C we determined the aggregation constants *K* and the corresponding Gibbs energy changes $\Delta G°$ (Table 4). It should be noted that **1a** and **1b** are not soluble in polar solvents such as alcohols, and **1c** is not soluble in non-polar solvents such as MCH. Nevertheless, the individual data sets are clearly connected because for a sufficient number of solvents of intermediate polarity accurate *K* values could be determined for two or even three of these compounds. All the *K* values are obtained by fitting of the UV/Vis spectral data according to the isodesmic (equal *K*) model[1c,27] with nonlinear least-square regression analysis. In all organic solvents applied here, the UV/Vis spectroscopic data could be fitted excellently with the isodesmic model, as illustrated in Fig. 5 for dyes **1b** and **1c**. In aqueous solution, even at very low concentrations (2×10^{-8} M) the UV/Vis spectrum only shows a slight change of shape from that at high concentration (10^{-4} M), indicating that the dye is still strongly aggregated at the most diluted conditions. Thus, one can only estimate a $K > 10^8$ M^{-1} in water, but the value can not be precisely determined.

According to Table 4, the magnitude of the aggregation constants *K* and corresponding Gibbs free energy changes $\Delta G° = -RT\ln K$ of the aggregation process of PBIs is highly solvent-dependent, indicating that the solvent polarity plays an important role for the thermodynamic stability of the aggregates. The difference between the smallest and largest *K* values can be six orders of magnitude. For the least polar solvents such as *n*-hexane or MCH the aggregation constants are large. In solvents of intermediate polarity and in particular those with high polarizability (CH_2Cl_2, $CHCl_3$) the *K* values become relatively small. For instance, for **1a** *K* drops down from 1.5×10^7 M^{-1} in MCH to 260 M^{-1} in $CHCl_3$. However, when the polarity of the solvent is further increased, the aggregation constants become larger again, as observed for **1c** in alcohols or water. Of particular importance for this study is the observation that the solvent-dependency of *K* is not influenced significantly by the solubilizing long alkyl or oligoethylene glycol side chains, *i.e.* almost

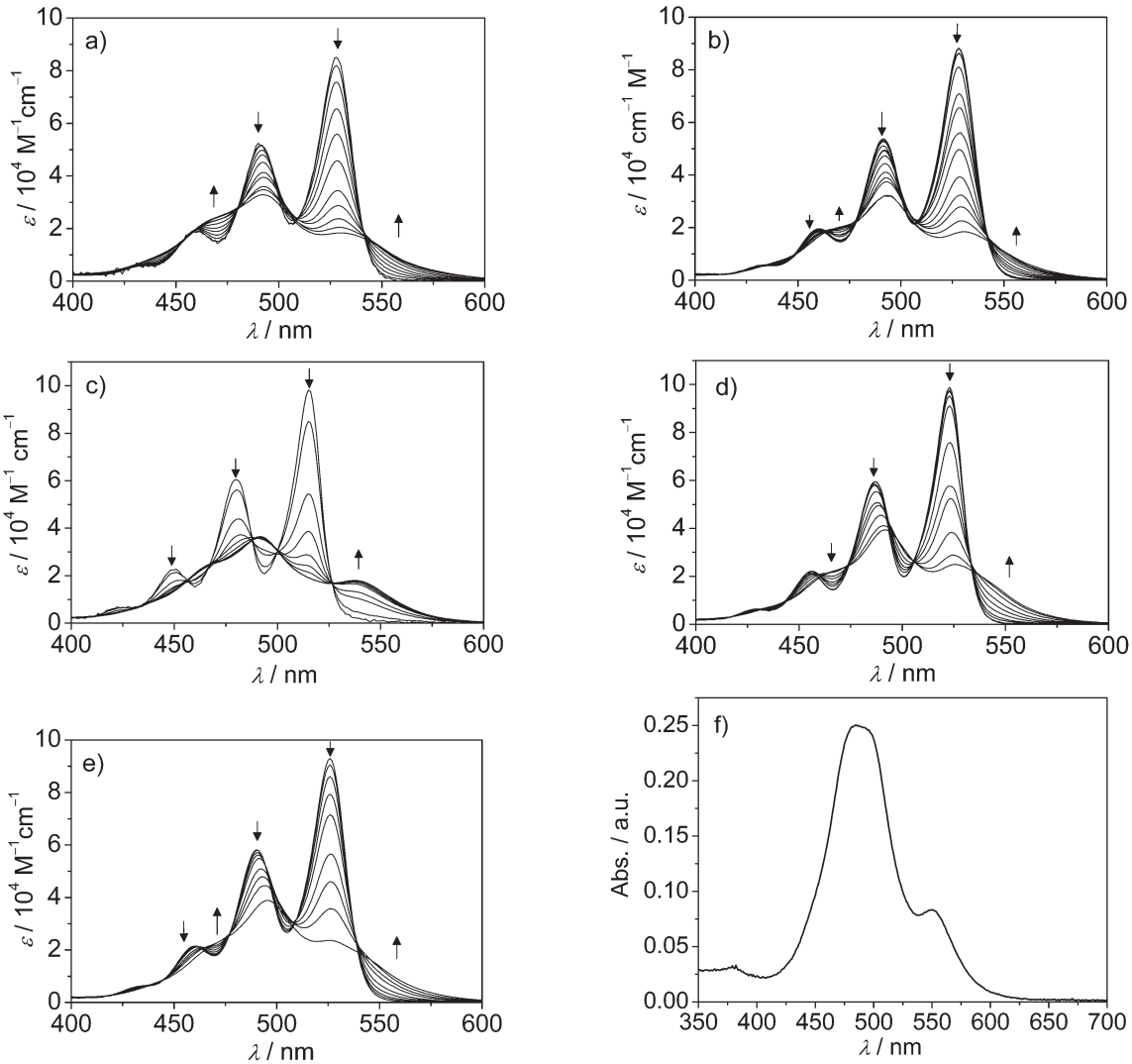

Fig. 4 Concentration-dependent UV/Vis spectra of (a) **1a** in toluene (1.0×10^{-7} M to 1.0×10^{-3} M), (b) **1b** in toluene (1.0×10^{-6} M to 2.2×10^{-2} M), (c) **1b** in *n*-hexane (2.2×10^{-7} M to 2.2×10^{-4} M), (d) **1b** in CCl_4 (5.1×10^{-7} M to 1.0×10^{-2} M), (e) **1c** in MeCN (2.2×10^{-6} M to 2.2×10^{-3} M), and (f) spectrum of **1c** in aqueous solution (9.1×10^{-6} M) at 25 °C. The arrows indicate the spectral changes upon increasing concentrations.

identical binding constants are obtained for **1b** and **1c** in all those solvents where values for both dyes could be determined (diethyl ether, CCl_4, toluene and THF). As a consequence of this range of data overlap the two data sets merge into one allowing coverage of the complete polarity range from *n*-hexane to water for this class of dyes. Also the solvent effect on the aggregation constant observed for **1a** complies well with those for **1b** and **1c** although the binding constants of **1a** are always about two orders of magnitude larger (see discussion on substituent effects above).

Linear free energy relationships (LFER)

The solvent effects on the Gibbs free energy $\Delta G°$ for the π–π stacking of the PBI dyes were evaluated by means of linear free energy relationships (LFER) with common solvent polarity parameters.[26] First, the Gibbs free energies for PBI aggregation were correlated with the relative permittivity ε_r and the Kirkwood–Onsager function $(\varepsilon_r - 1)/(2\varepsilon_r + 1)$ which have distinct physical meaning and only consider the contribution of electrostatic interactions.[17,26] For compound **1a**, a rather good linear correlation with the simple parameter ε_r can be observed (Fig. 6a, correlation coefficient $r = 0.97$) if the three solvents with the highest refractive index, *i.e.* CCl_4, toluene and $CHCl_3$ are not included in the fitting procedure. With increasing ε_r, the values of $-\Delta G°$ decrease nearly linearly in the five solvents whose polarity is dominated by dipolarity and not by polarizability, indicating that electrostatic interactions between PBI dyes **1a** play a crucial role for the π–π stacking strength. Similar trends can be observed by using the Kirkwood–Onsager function instead of ε_r, however, the correlation coefficient decreases to 0.86 (Fig. 7). In contrast, the aggregation of **1c** in polar solvents can not be described in a reasonable way by these electrostatic parameters although the applied solvents have relatively low polarizability except DMSO (Fig. 6b). For the four alcoholic solvents, a steady increase of the values of $-\Delta G°$ can be observed

upon increasing ε_r. This trend also points towards the extremely high $-\Delta G°$ value of >45 kJ mol^{-1} in water (ε_r = 78). The data points for other solvents, however, deviate largely from those of the alcoholic solvents.

These results indicate that electrostatic forces are not sufficient to explain the π–π stacking of PBI dyes. Because both electrostatic and dispersion interactions are important for a reasonable description of the π–π stacking of PBI dyes, empirical solvent polarity scales including $E_T(30)$,[26] π^*[30] as well as χ_R[31] were applied in the next step of our study. The less common latter scale was established by Brooker *et al.* based on the solvatochromism of a polymethine dye.[31] These scales have been shown to exhibit different sensitivities towards dipolarity and polarizability contributions as well as towards additional specific interactions like hydrogen bonding of the solute with the solvent.

Table 3 Wavelengths of the absorption maxima of the monomer and aggregate bands of PBIs **1a–c** in various solvents at 25 °C

Solvent	**1a** λ_{mon}/nm	**1a** λ_{agg}/nm	**1b** λ_{mon}/nm	**1b** λ_{agg}/nm	**1c** λ_{mon}/nm	**1c** λ_{agg}/nm
n-Hexane	[a]		515	492	[a]	[a]
MCH	517	491	517	492	[a]	[a]
Di-*n*-butyl ether	520	494	522	494	[a]	[a]
Diethyl ether	518	492	518	489	518	490
CCl_4	524	491	523	492	523	491
Toluene	528	492	528	493	527	[b]
THF	523	493	522	[b]	521	[b]
CH_2Cl_2	527	492	527	[b]	526	[b]
$CHCl_3$	529	494	528	[b]	527	[b]
Acetone	[a]		[a]		519	490
CH_3CN	[a]		[a]		526	495
DMSO	[a]		[a]		533	500
n-Butanol	[a]		[a]		526	493
n-Propanol	[a]		[a]		526	493
EtOH	[a]		[a]		524	492
MeOH	[a]		[a]		525	493
H_2O	[a]		[a]		[c]	485

[a] Not sufficiently soluble at room temperature. [b] No accurate data could be determined. [c] The monomer band of **1c** can not be observed in water.

Our analyses revealed reasonably good linear correlations between the solvent-dependent $-\Delta G°$ values for PBI aggregation and empirical solvent polarity parameters χ_R and π^* if one excludes the solvents with the highest refractive index values and accordingly high polarizability contributions, such as CCl_4 and DMSO. In these solvents, the π–π aggregation constants significantly drop down and deviate from the linear correlation. Fig. 8a shows the correlation of the Gibbs aggregation energies of **1a** in eight solvents with χ_R scale. An excellent linear free energy relationship was observed for the solvents if CCl_4 was excluded (correlation coefficient r = 0.98). The correlation is obviously improved in comparison with that obtained for ε_r.

For **1b**, the correlation line is nearly parallel with the line for **1a** (circles in Fig. 8b, r = 0.92), indicating that the solvent polarity has almost identical effects on the Gibbs aggregation free energy for both dyes and the difference of the magnitude of K value mainly originates from the structural differences of the two compounds (see above). For **1c** (triangles in Fig. 8b, r = 0.89), notably, if solvents of high polarizability and Et_2O are excluded, an increase of $-\Delta G°$ was observed upon increasing the solvent polarity, which is clearly the opposite trend to that observed for **1a** and **1b**.

Good linear correlation of the Gibbs aggregation energies can also be observed with the π^* scale. As shown in Fig. 9a, linear correlation can be obtained for the $-\Delta G°$ values of PBI dyes **1a** and **1b** with this polarity scale. The dye **1a** shows the best fitting with a correlation coefficient r = 0.98. Again, the lines for **1a,b** obtained from linear regression are nearly parallel. On the other hand, this scale does not correlate with the Gibbs aggregation energies of **1c** in the more polar solvents, as shown in Fig. 9b. This behaviour is similar with that observed in Fig. 6b, which is obtained for ε_r scale.

For the $E_T(30)$ good linear correlation can be obtained for PBI **1a** (r = 0.98, Fig. 10a) in the low polarity solvents if the three

Table 4 Aggregation constants K and corresponding Gibbs free energy changes $\Delta G°$ of PBIs **1a–c** in various solvents at 25 °C

Solvent	**1a** K/M^{-1}	**1a** $-\Delta G°$/kJ mol^{-1}	**1b** K/M^{-1}	**1b** $-\Delta G°$/kJ mol^{-1}	**1c** K/M^{-1}	**1c** $-\Delta G°$/kJ mol^{-1}
n-Hexane	[a]		1.2×10^6	34.7	[a]	
MCH	1.5×10^7	40.9	9.7×10^4	28.4	[a]	
Di-*n*-butyl ether	3.0×10^6	36.9	2.9×10^4	25.4	[a]	
Diethyl ether	3.6×10^6	37.3	3.3×10^4	25.7	3.1×10^4	25.3
CCl_4	1.8×10^5	30.0	6.5×10^2	16.0	1.4×10^3	17.9
Toluene	4.5×10^4	26.5	5.9×10^2	15.8	5.7×10^2	15.8
THF	5.4×10^4	27.0	2.7×10^2	13.9	2.5×10^2	13.7
CH_2Cl_2	1.6×10^3	18.3	[b]		[b]	
$CHCl_3$	2.6×10^2	13.8	[b]		[b]	
DMSO	[a]		[a]		9.9×10^2	17.1
Acetone	[a]		[a]		3.2×10^3	20.0
CH_3CN	[a]		[a]		5.5×10^3	21.3
n-Butanol	[a]		[a]		1.5×10^4	23.8
n-Propanol	[a]		[a]		2.9×10^4	25.4
EtOH	[a]		[a]		4.0×10^4	26.2
MeOH	[a]		[a]		5.3×10^4	26.9
H_2O	[a]		[a]		$>10^8$	>45

[a] Not sufficiently soluble. [b] No accurate data could be determined because the small binding constant (K < 20 M^{-1}) demands highly concentrated solutions with too high optical densities.

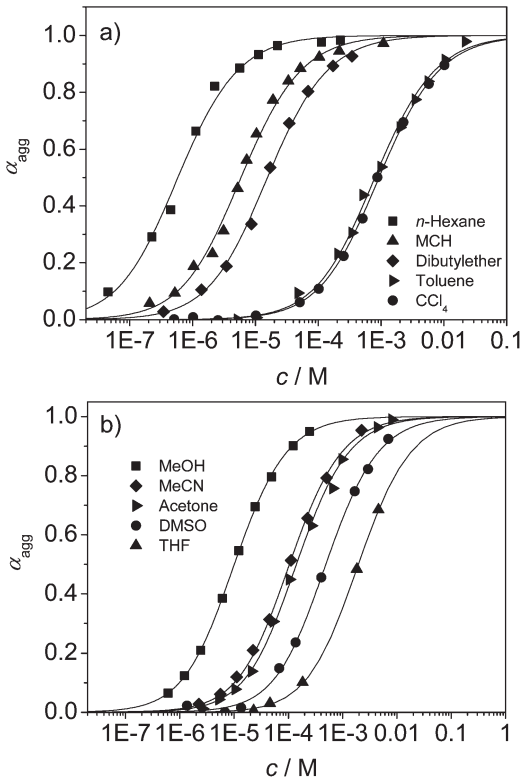

Fig. 5 Molar fraction of aggregated molecules α_{agg} as a function of concentration of the PBI dyes in different solvents: (a) for dye **1b** and (b) for dye **1c**. The curves were obtained by fitting the concentration-dependent UV/Vis data with the isodesmic model.

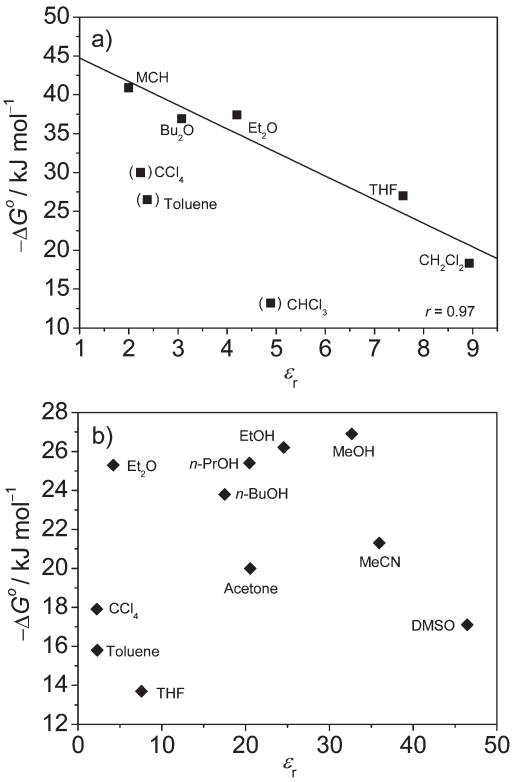

Fig. 6 (a) Plot of $-\Delta G°$ of dye **1a** *vs.* relative permittivity ε_r of different solvents. The data points for $CHCl_3$, CCl_4 and toluene are not included for the linear fitting. (b) Plot of $-\Delta G°$ of **1c** *vs.* relative permittivity ε_r.

solvents CCl_4, toluene, and $CHCl_3$ (low dipolarity but high polarizability) are excluded. In comparison with the χ_R and π^* scales (Fig. 8a and 9a) more solvents had to be excluded for achieving a reasonable linear correlation to $E_T(30)$ scale, indicating that the latter is more sensitive to the polarizability of the solvents. If diethyl ether, CCl_4 and DMSO are excluded, also an excellent linear correlation is observed between the $-\Delta G°$ values for **1c** and the $E_T(30)$ values of the polar solvents (Fig. 10b). Notably, the solvents used for **1c** are almost identical to those applied by Smithrud and Diederich[12] and Cubberley and Iverson,[16] respectively, in their investigations of the solvent effect on molecular complexes of aromatic compounds. Like for their cyclophane–pyrene and dialkoxynaphthalene–naphthalene diimide systems also for PBI aggregates an increase of $-\Delta G°$ is observed with increasing $E_T(30)$ solvent polarity. In contrast to the previously studied aggregate systems, however, PBI aggregation in water is governed by an unusually strong hydrophobic effect (Fig. 9b and 10b) which motivates further studies that are currently performed in our laboratory.

As discussed by Hunter and Sanders,[10] the forces contributing to π–π interactions include electrostatic interactions between the static charge distributions of the π-conjugated molecules, London dispersion forces, solvophobic effects and charge transfer (CT) interactions. The observed solvent effects on the π–π aggregation of PBIs, *i.e.* the decrease of the aggregation constants with increasing polarity of the solvents for **1a** and **1b**, and the opposite trends in the more polar solvents for **1c** clearly

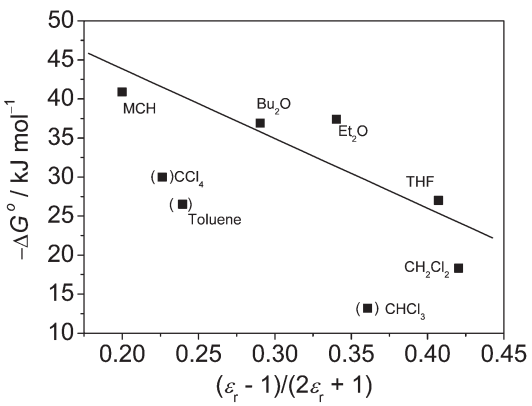

Fig. 7 Plot of $-\Delta G°$ of dye **1a** *vs.* Kirkwood–Onsager function $(\varepsilon_r - 1)/(2\varepsilon_r + 1)$ of different solvents. The data points for $CHCl_3$, CCl_4 and toluene are not included for the linear fitting.

suggest that the π–π stacking forces between PBIs are dominated by different interactions in different solvents.

The solvent dependency of the aggregation constants of **1a** and **1b** indicate that electrostatic forces provide an important contribution to the π–π stacking strength in particular in nonpolar media. Accordingly, to rationalize the LFER relationships between the $-\Delta G°$ values of these dyes and χ_R and π^* scales, beyond general electrostatic interactions between polycyclic aromatic hydrocarbons also quadrupole–quadrupole interactions

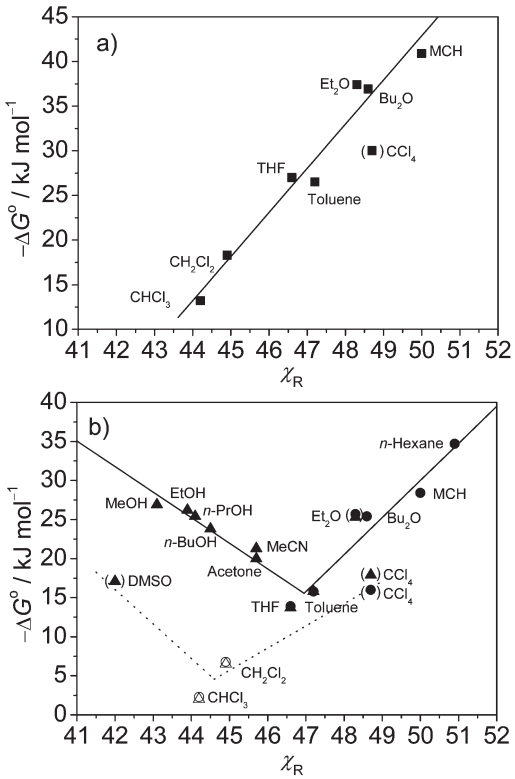

Fig. 8 Plots of $-\Delta G°$ *vs.* the χ_R solvent polarity scale for (a) **1a** (square, correlation coefficient $r = 0.98$), (b) **1b** (circles, $r = 0.92$) and **1c** (triangles, $r = 0.89$). The data points for **1b** and **1c** in CCl_4 and for **1c** in DMSO and Et_2O are not included in the linear regression analyses (solid lines). For **1b,c** in the solvents of high polarizability two additional linear regression analyses (for **1b** in CCl_4, CH_2Cl_2 and $CHCl_3$ and for **1c** in DMSO, CH_2Cl_2 and $CHCl_3$) were performed (dotted lines). The values in CH_2Cl_2 and $CHCl_3$ (empty circles and triangles) are estimated by LFER from the values obtained for **1a** in these solvents.

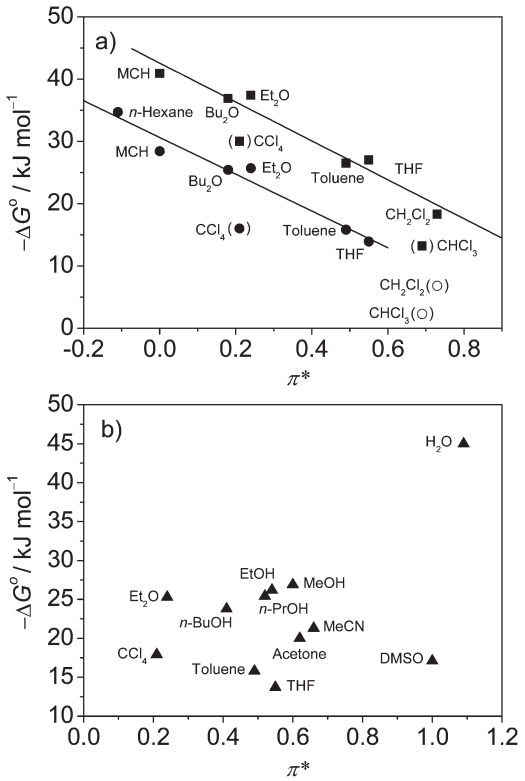

Fig. 9 Plot of $-\Delta G°$ *vs.* the π^* solvent polarity scale for (a) **1a** (squares, correlation coefficient $r = 0.98$) and **1b** (circles, $r = 0.96$), and (b) **1c** (triangles). In (a), the values for **1b** in CH_2Cl_2 and $CHCl_3$ (empty circles) are estimated by LFER from the values obtained for **1a** in these solvents and are not included in regression analysis. The data points for CCl_4 and $CHCl_3$ are not included in the linear regression analysis in (a), and the data point for H_2O in (b) is only a lower limit.

between PBI dyes or local electrostatic attractive forces between dipolar elements within PBI dyes (*e.g.* carbonyl groups) might be effective. These specific electrostatic interactions may also explain why PBI dyes are among the most strongly aggregating π-systems[1c] and why electron-rich groups at the phenyl substituent in imide position (**1a**) afford a substantial increase of the aggregation constants.

However, the fact that the aggregation constants drop down drastically in the most polarizable solvents and that no good correlations between the Gibbs aggregation energy $\Delta G°$ and the Kirkwood–Onsager function could be observed is in contrast to the results obtained for dipolar merocyanine dyes.[17] For these dyes the aggregation appears to be dominated by electrostatic interactions over a much wider range of solvents owing to the large dipole moment of these dyes. Quadrupolar interactions[32] are weaker and the π-system of PBI is larger. Accordingly dispersion forces gain weight and highly polarizable solvents like CCl_4 effect a more significant drop of the aggregation constant owing to its capability to replace the solute–solute by similarly strong solute–solvent interactions.

Whilst so far data for aliphatic, aromatic, chloroaliphatic and the less dipolar solvents could be rationalized, the data in highly dipolar solvents and structured solvents, *i.e.* alcohols and water, are more difficult to explain. The increase of the aggregation constants upon increasing the solvent polarity for alcohols and the extremely large aggregation constant in aqueous solution for **1c** indicate that another contribution is operative in these solvents. The two LFERs for **1b** and **1c** depicted in Fig. 8b appear to be most suitable for further elucidation of the solvent effects upon PBI aggregation. For four solvents (Et_2O, CCl_4, toluene, THF) almost equal aggregation constants could be determined for **1b** and **1c** which suggests that the side chains (alkyl *vs.* oligoethylene glycol) do not contribute significantly to the observed solvent dependencies of the aggregation constants. Accordingly, both regression lines in Fig. 8b may be merged together to get the full picture on the thermodynamics of PBI aggregation over the complete solvent polarity range. As a consequence we can conclude that the π–π stacking interactions between PBIs are at a minimum for solvents of intermediate polarity, *i.e.* THF and toluene. As already noted before, solvents of similar dipolarity but higher polarizability weaken the attractive interactions between the PBI dyes. For this reason the aggregation constants in CH_2Cl_2 and $CHCl_3$ are not accessible anymore from UV/Vis experiments for dyes **1b,c** but can be estimated to be around 14 M^{-1} and 2 M^{-1}, respectively, by LFER from the values obtained for **1a** in these solvents (these values are used for the plot in Fig. 8b and are also embedded in Fig. 9a). If the solvent polarity is reduced (data on the right side

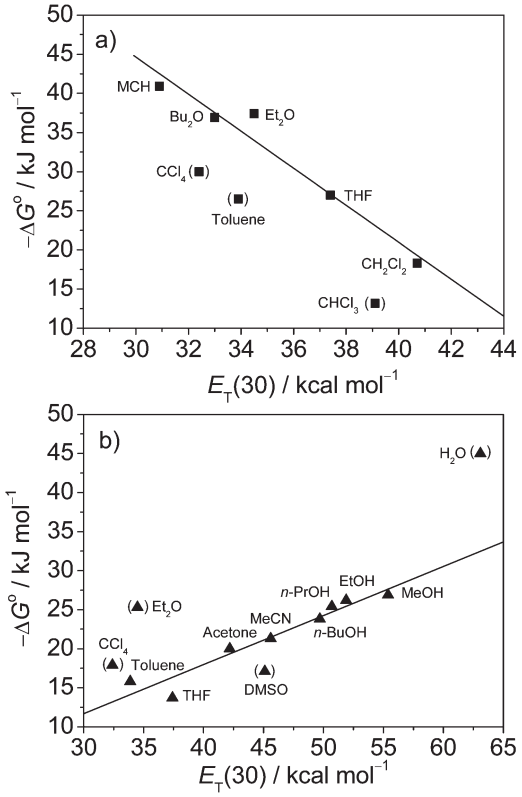

Fig. 10 Plot of $-\Delta G°$ *vs.* the $E_T(30)$ solvent polarity scale for (a) **1a** (squares, correlation coefficient $r = 0.98$, the data points for CCl_4, toluene, and $CHCl_3$ are not included for the linear regression analysis), (b) **1c** (triangles, $r = 0.92$, the data points for Et_2O, CCl_4, DMSO and the estimated lower limit for H_2O are not included in the linear regression analysis). Note that for MCH no $E_T(30)$ value is available and the value of cyclohexane was used instead in (a).

of the minimum in Fig. 8b) a steady increase of $-\Delta G°$ is observed pointing at the prevalence of electrostatic attractions between quadrupolar PBI dyes in the nonpolar solvents. In contrast, the increase of $-\Delta G°$ for the polar solvents (data on the left side from the minimum in Fig. 8b) can obviously not be explained by electrostatic interactions that are already too weak to trigger self-assembly of PBIs in environments of intermediate polarity like THF. In these polar solvents aggregation appears to be governed by solvophobic contributions. If the solvent like in the case of the highly polarizable DMSO is able to solvate the PBI solute by strong dispersion interactions, $-\Delta G°$ values remain low. If this is not the case as demonstrated in particular for the protic alcoholic solvents and water, stacking of PBI dyes becomes driven by dispersion interactions between the extended π-conjugated scaffolds leading to an increase of $-\Delta G°$.

In compliance with the strong dispersion interactions arising between extended π-scaffolds, the reduced binding strength between PBI dyes in all highly polarizable solvents DMSO, CH_2Cl_2, $CHCl_3$ and CCl_4 can be attributed to improved dispersion interactions between solute and solvent molecules. This solvent effect which is related to its refractive index can be accounted for by an (empirical) offset of both regression lines as illustrated by the dotted lines in Fig. 8b.

Conclusions

The solvents and the substituents attached at the imide groups are two important factors that influence the π–π aggregation of PBIs. In the case of phenyl substituents at the imide positions sterical (**1f**) as well as electronic factors (**1a**) were demonstrated to have a significant impact on the aggregation constants and the corresponding Gibbs free aggregation energies. Equally important, however, is the impact of the solvent. By collecting data in 17 solvents with different dipolarity, polarizability and hydrogen bond donor and acceptor capabilities for the three structurally related PBI dyes **1a–c** we could show that the magnitude of the π–π interactions between PBI dyes is modulated significantly by the solvent. LFER analyses with common empirical solvent polarity scales revealed a biphasic behaviour, *i.e.* a decrease of the aggregation constant for PBIs with increasing solvent polarity for aliphatic and dipolar aprotic solvents up to solvents of intermediate polarity (THF, toluene) and a subsequent increase of the aggregation constant with increasing solvent polarity for strongly dipolar and protic solvents and in particular for water. The smallest propensity for PBI aggregation is found for highly polarizable chlorinated solvents of intermediate polarity, *i.e.* CH_2Cl_2 and $CHCl_3$.

These results could be rationalized by different solvation effects that compete with the intermolecular forces involved in the π–π stacking of PBIs to a different extent in the respective solvents. Thus, the impact of electrostatic, dispersion and solvophobic forces on the aggregation of PBIs appears to alter considerably over the whole solvent polarity scale, depending on the nature of the respective solvent. For protic solvents, solvophobic effects provide a reasonable explanation but additional specific effects arising from hydrogen bonding between the solvent molecules and the carbonyl oxygens of the PBIs might also play a role. In particular the enormous increase of the aggregation constant in water that we related in this study in a rather superficial manner to the "hydrophobic effect" warrants further experimental work.

Experimental section

General methods

All solvents and reagents were purchased from commercial sources and used as received. Compounds **1a**, **1b** and **1e** were prepared according to the literature.[21a,e,24a] Perylene bisimide **1f** was obtained from BASF SE. Perylene-3,4 : 9,10-tetracarboxylic acid bisanhydride was obtained from Aldrich. NMR spectra were recorded at 298 K on Bruker 400 MHz spectrometer and all the spectra were calibrated with TMS. The solvents for spectroscopic studies were of spectroscopic grade and used as received. UV/Vis spectra were measured in cells with pathlengths between 0.01 mm and 1 cm on a Perkin Elmer Lambda 40P spectrometer equipped with a Peltier system as the temperature controller. The steady state fluorescence spectra were measured on a PTI QM4/2003 spectrofluorometer. The fluorescence quantum yields were determined by the optically dilute method by using fluorescein (Φ_{em} = 0.92 in 1 N aqueous NaOH) and *N*,*N*′-bis(2,6-diisopropylphenyl)perylene-3,4:9,10-tetracarboxylic acid bisimide **1f** (Φ_{em} = 1.00 in $CHCl_3$), as standards. The reported quantum

yields are averaged values obtained at three different excitation wavelengths for each PBI.

Aggregation studies by UV/Vis spectroscopy

The UV/Vis spectra of compounds **1a–f** were recorded at different concentrations at 25 °C. The apparent molar absorption coefficients at suitable wavelengths were fitted by nonlinear least-square regression analysis to the isodesmic (equal *K*) model.[1c,27] The aggregation constants *K* and corresponding Gibbs free energy changes are averaged values (error < ± 1.0 kJ mol^{-1}) obtained at three different wavelengths (difference between selected wavelengths >25 nm). The degree (or fraction) of aggregated molecules α_{agg} can be written as $\alpha_{agg} = 1 - c_1/c_T$, where c_1 is the concentration of the monomer and c_T is the total concentration of the compound. The degree of aggregated molecules can be obtained according to the following equation:[1c]

$$a_{agg} = 1 - \frac{2Kc_T + 1 - \sqrt{4Kc_T + 1}}{2K^2c_T^2}$$

N,*N*′-Bis[3,4,5-tri(3-{2-[2-(ethoxy)ethoxy]ethoxy}propyl)phenyl] perylene-3,4:9,10-tetracarboxylic acid bisimide (1c)

Perylene-3,4:9,10-tetracarboxylic acid bisanhydride (0.13 g, 0.33 mmol), 3,4,5-tri(3-{2-[2-(ethoxy)ethoxy]ethoxy}propyl) aniline (0.40 g, 0.67 mmol) and zinc acetate (0.073 g, 0.33 mmol) were mixed with 5.0 g of imidazole. The reaction mixture was stirred at 150 °C for 6 h. After cooling to room temperature, 30 mL of 2 N hydrochloride acid was added to the mixture. The solution was extracted with 50 mL dichloromethane three times. The combined dichloromethane solution was dried with anhydrous $MgSO_4$ and then the solvent was evaporated. The crude product was further purified by silica gel column chromatography (CH_2Cl_2–ethyl acetate–MeOH, 90 : 8 : 2 as eluent) to give 280 mg (56%) of pure product. ^{1}H NMR (400 MHz, $CDCl_3$): δ 8.75 (d, 4H, J = 8.0 Hz, H_{pery}), 8.70 (d, 4H, J = 8.2 Hz, H_{pery}), 7.01 (s, 4H, Ar–H), 3.7–3.4 (m, 72H, OCH_2), 2.9–2.6 (m, 12H, $ArCH_2$), 2.0–1.8 (m, 12H, CH_2), 1.1–1.3 (m, 18H, CH_3). MS (FAB, matrix: *p*-octyloxynitrobenzene) calculated for $C_{90}H_{126}N_2O_{22}$, 1586.9 *m*/*z*, found 1588.2 $[M + H]^+$; MS (MALDI-TOF, matrix: DTCB) calculated for $C_{90}H_{126}N_2O_{22}$, 1586.9 *m*/*z*, found 1586.8 $[M]^+$; elemental analysis (%) calculated for $C_{90}H_{126}N_2O_{22}$: C 68.07, H 8.00, N 1.76; found: C 67.43, H 8.10, N 1.67; UV/Vis (CH_2Cl_2): $\lambda_{max}(\varepsilon)$ = 527 (96 400), 490 (58 100), 459 (21 200), 434 (6200), 369 nm (5000 M^{-1} cm^{-1}).

N,*N*′-Di(2-*n*-hexyldecyl)perylene-3,4:9,10-tetracarboxylic acid bisimide (1d)

In a 25 mL flask were placed perylene-3,4:9,10-tetracarboxylic acid bisanhydride (0.102 g, 0.26 mmol), 2-*n*-hexyldecan-1-amine (0.13 g, 0.54 mmol) and 1.59 g of imidazole under an argon atmosphere. The mixture was heated to 180 °C and stirred for 4 h. After cooling to RT the reaction mixture was diluted with dichloromethane and washed with 2 N hydrochloride acid, water, saturated sodium bicarbonate solution and once more with water. The organic phase was then dried with anhydrous $MgSO_4$ and concentrated under reduced pressure. The crude product was purified by silica gel column chromatography (dichloromethane) to yield 187 mg (86%) of a red solid. ^{1}H NMR (400 MHz, CD_2Cl_2): δ 8.28–8.26 (d, J = 7.9 Hz, 4H, H_{pery}), 8.11–8.08 (d, J = 8.2 Hz, 4H, H_{pery}), 4.04–4.02 (d, J = 7.2 Hz, 4H, NCH_2), 1.95 (m, 2H, CH), 1.42–1.24 (m, 48H, CH_2), 0.86 (t, J = 6.5 Hz, 6H, CH_3), 0.84 (t, J = 7.0 Hz, 6H, CH_3); ^{13}C-NMR (100.6 MHz, CD_2Cl_2): δ 163.54, 134.03, 131.03, 129.17, 125.97, 123.41, 123.02, 44.93, 37.11, 32.36, 32.35, 32.18, 32.14, 30.54, 30.23, 30.07, 29.79, 26.92, 26.89, 23.12, 23.11, 14.30, 14.29; HRMS (ESI) calculated for $C_{56}H_{75}N_2O_4$, 839.573 *m*/*z*, found 839.572 $[M + H]^+$; elemental analysis (%) calculated for $C_{56}H_{74}N_2O_4$: C 80.15, H 8.89, N 3.34; found: C 79.95, H 9.32, N 3.24; UV/Vis ($CHCl_3$): $\lambda_{max}(\varepsilon)$ = 523 (85 600), 487 (51 300), 456 (18 400), 431 (5100), 368 nm (3700 M^{-1} cm^{-1}).

Acknowledgements

We gratefully acknowledge financial support of our work by the Deutsche Forschungsgemeinschaft (DFG) within the framework of the research training school GRK 1221 “Control of electronic properties in aggregates of π-conjugated molecules” at the Universität Würzburg.

Notes and references

‡ A part of the results reported in this paper have already been summarized in our recent review article, ref. 1*c*.

1 For reviews on the π–π stacking of aromatic molecules, see: (*a*) C. A. Hunter, K. R. Lawson, J. Perkins and C. J. Urch, *J. Chem. Soc., Perkin Trans. 2*, 2001, 651–669; (*b*) M. L. Waters, *Curr. Opin. Chem. Biol.*, 2002, **6**, 736–741; (*c*) Z. Chen, A. Lohr, C. R. Saha-Möller and F. Würthner, *Chem. Soc. Rev.*, 2009, **38**, 564–584.
2 (*a*) E. A. Meyer, R. K. Castellano and F. Diederich, *Angew. Chem., Int. Ed.*, 2003, **42**, 1210–1250; (*b*) J. W. Steed and J. L. Atwood, *Supramolecular Chemistry*, John Wiley & Sons, Chichester, 2000, pp. 26–28; (*c*) G. B. McGaughey, M. Gagné and A. K. Rappé, *J. Biol. Chem.*, 1998, **273**, 15458–15463.
3 (*a*) G. McDermott, S. M. Prince, A. A. Freer, A. M. Hawthornthwaite-Lawless, M. Z. Papiz, R. J. Cogdell and N. W. Isaacs, *Nature*, 1995, **374**, 517–521; (*b*) H. Tamiaki, *Coord. Chem. Rev.*, 1996, **148**, 183–197, and the literature cited therein; (*c*) X. Hu and K. Schulten, *Phys. Today*, 1997, **50**, 28–34; (*d*) T. S. Balaban, H. Tamiaki and A. R. Holzwarth, *Top. Curr. Chem.*, 2005, **258**, 1–38.
4 (*a*) P. W. Bohn, *Annu. Rev. Phys. Chem.*, 1993, **44**, 37–60; (*b*) F. Würthner, T. E. Kaiser and C. R. Saha-Möller, *Angew. Chem., Int. Ed.*, 2011, **50**, 3376–3410.
5 (*a*) P. Terech and R. G. Weiss, *Chem. Rev.*, 1997, **97**, 3133–3159; (*b*) T. Ishi-i and S. Shinkai, *Top. Curr. Chem.*, 2005, **258**, 119–160; (*c*) A. Ajayaghosh and V. K. Praveen, *Acc. Chem. Res.*, 2007, **40**, 644–656.
6 (*a*) A. N. Cammidge and R. J. Bushby in *Handbook of Liquid Crystals, Vol. 2B: Low Molecular Weight Liquid Crystals II*, ed. D. Demus, J. Goodby, G. W. Gray, H.-W. Spiess and V. Vill, Wiley-VCH, Weinheim, 1998, pp. 693–743; (*b*) S. Sergeyev, W. Pisula and Y. H. Geerts, *Chem. Soc. Rev.*, 2007, **36**, 1902–1929.
7 A. P. H. J. Schenning and E. W. Meijer, *Chem. Commun.*, 2005, 3245–3258.
8 (*a*) M. R. Wasielewski, *Acc. Chem. Res.*, 2009, **42**, 1910–1921; (*b*) N. Sakai, A. L. Sisson, S. Bhosale, A. Fürstenberg, N. Banerji, E. Vauthey and S. Matile, *Org. Biomol. Chem.*, 2007, **5**, 2560–2563.
9 (*a*) D. T. McQuade, A. E. Pullen and T. M. Swager, *Chem. Rev.*, 2000, **100**, 2537–2574; (*b*) L. Chen, D. W. McBranch, H.-L. Wang, R. Helgeson, F. Wudl and D. G. Whitten, *Proc. Natl. Acad. Sci. U. S. A.*, 1999, **96**, 12287–12292.

10 (*a*) C. A. Hunter and J. K. M. Sanders, *J. Am. Chem. Soc.*, 1990, **112**, 5525–5534; (*b*) C. A. Hunter, *Chem. Soc. Rev.*, 1994, **23**, 101–109.
11 (*a*) S. Grimme, J. Antony, T. Schwabe and C. Mück-Lichtenfeld, *Org. Biomol. Chem.*, 2007, **5**, 741–758; (*b*) S. Grimme, *Angew. Chem., Int. Ed.*, 2008, **47**, 3430–3434.
12 (*a*) D. B. Smithrud and F. Diederich, *J. Am. Chem. Soc.*, 1990, **112**, 339–343; (*b*) D. B. Smithrud, T. B. Wyman and F. Diederich, *J. Am. Chem. Soc.*, 1991, **113**, 5420–5426; (*c*) F. Diederich, *Angew. Chem., Int. Ed. Engl.*, 1988, **27**, 362–386.
13 For other examples for LFER analyses of solvent effects in supramolecular chemistry, see: (*a*) H.-J. Schneider, R. Kramer, S. Simova and U. Schneider, *J. Am. Chem. Soc.*, 1988, **110**, 6442–6448; (*b*) G. A. Breault, C. A. Hunter and P. C. Mayers, *J. Am. Chem. Soc.*, 1998, **120**, 3402–3410; (*c*) J. Schmidt, R. Schmidt and F. Würthner, *J. Org. Chem.*, 2008, **73**, 6355–6362.
14 (*a*) F. J. M. Hoeben, P. Jonkheijm, E. W. Meijer and A. P. H. J. Schenning, *Chem. Rev.*, 2005, **105**, 1491–1546; (*b*) D. J. Hill, M. J. Mio, R. B. Prince, T. S. Hughes and J. S. Moore, *Chem. Rev.*, 2001, **101**, 3893–4012.
15 L. Zang, Y. Che and J. S. Moore, *Acc. Chem. Res.*, 2008, **41**, 1596–1608.
16 M. S. Cubberley and B. L. Iverson, *J. Am. Chem. Soc.*, 2001, **123**, 7560–7563.
17 (*a*) F. Würthner, S. Yao, T. Debaerdemaeker and R. Wortmann, *J. Am. Chem. Soc.*, 2002, **124**, 9431–9447; (*b*) F. Würthner and S. Yao, *Angew. Chem., Int. Ed.*, 2000, **39**, 1978–1981.
18 (*a*) A. S. Shetty, J. Zhang and J. S. Moore, *J. Am. Chem. Soc.*, 1996, **118**, 1019–1027; (*b*) S. Lahiri, J. L. Thompson and J. S. Moore, *J. Am. Chem. Soc.*, 2000, **122**, 11315–11319.
19 M. Kastler, W. Pisula, D. Wasserfallen, T. Pakula and K. Müllen, *J. Am. Chem. Soc.*, 2005, **127**, 4286–4296.
20 For reviews, see ref. 8*a* and: (*a*) F. Würthner, *Chem. Commun.*, 2004, 1564–1579; (*b*) C. Huang, S. Barlow and S. R. Marder, *J. Org. Chem.*, 2011, **76**, 2386–2407; (*c*) F. Würthner and M. Stolte, *Chem. Commun.*, 2011, **47**, 5109–5115; (*d*) X. Zhan, A. Facchetti, S. Barlow, T. J. Marks, M. A. Ratner, M. R. Wasielewski and S. R. Marder, *Adv. Mater.*, 2011, **23**, 268–284.
21 (*a*) F. Würthner, C. Thalacker, S. Diele and C. Tschierske, *Chem.–Eur. J.*, 2001, **7**, 2245–2253; (*b*) J. van Herrikhuyzen, A. Syamakumari, A. P. H. J. Schenning and E. W. Meijer, *J. Am. Chem. Soc.*, 2004, **126**, 10021–10027; (*c*) Z. An, J. Yu, S. C. Jones, S. Barlow, S. Yoo, B. Domercq, P. Prins, L. D. A. Siebbeles, B. Kippelen and S. R. Marder, *Adv. Mater.*, 2005, **17**, 2580–2583; (*d*) F. Würthner, Z. Chen, V. Dehm and V. Stepanenko, *Chem. Commun.*, 2006, 1188–1190; (*e*) Z. Chen, V. Stepanenko, V. Dehm, P. Prins, L. D. A. Siebbeles, J. Seibt, P. Marquetand, V. Engel and F. Würthner, *Chem.–Eur. J.*, 2007, **13**, 436–449; (*f*) X. Zhang, Z. Chen and F. Würthner, *J. Am. Chem. Soc.*, 2007, **129**, 4886–4887; (*g*) M. R. Hansen, T. Schnitzler, W. Pisula, R. Graf, K. Müllen and H. W. Spiess, *Angew. Chem., Int. Ed.*, 2009, **48**, 4621–4624; (*h*) A. Wicklein, A. Lang, M. Muth and M. Thelakkat, *J. Am. Chem. Soc.*, 2009, **131**, 14442–14453.
22 (*a*) J. Seibt, P. Marquetand, V. Engel, Z. Chen, V. Dehm and F. Würthner, *Chem. Phys.*, 2006, **328**, 354–362; (*b*) J. Seibt, V. Dehm, F. Würthner and V. Engel, *J. Chem. Phys.*, 2007, **126**, 164308-1–164308-6; (*c*) R. Fink, J. Seibt, V. Engel, M. Renz, M. Kaupp, S. Lochbrunner, H.-M. Zhao, J. Pfister, F. Würthner and B. Engels, *J. Am. Chem. Soc.*, 2008, **130**, 12858–12859; (*d*) H.-M. Zhao, J. Pfister, V. Settels, M. Renz, M. Kaupp, V. C. Dehm, F. Würthner, R. F. Fink and B. Engels, *J. Am. Chem. Soc.*, 2009, **131**, 15660–15668.
23 G. Seybold and G. Wagenblast, *Dyes Pigm.*, 1989, **11**, 303–317.
24 (*a*) H. Langhals, S. Demmig and T. Potrawa, *J. Prakt. Chem.*, 1991, **333**, 733–748; (*b*) H. Langhals, *Heterocycles*, 1995, **40**, 477–500; (*c*) H. Langhals, J. Karolin and L. B.-Å. Johansson, *J. Chem. Soc., Faraday Trans.*, 1998, **94**, 2919–2922.
25 E. H. A. Beckers, S. C. J. Meskers, A. P. H. J. Schenning, Z. Chen, F. Würthner and R. A. J. Janssen, *J. Phys. Chem. A*, 2004, **108**, 6933–6937.
26 C. Reichardt, *Solvents and Solvent Effects in Organic Chemistry*, Wiley-VCH, Weinheim, 2003.
27 R. B. Martin, *Chem. Rev.*, 1996, **96**, 3043–3064.
28 L. D. Wescott and D. L. Mattern, *J. Org. Chem.*, 2003, **68**, 10058–10066.
29 W. Wang, W. Wan, H.-H. Zhou, S. Niu and A. D. Q. Li, *J. Am. Chem. Soc.*, 2003, **125**, 5248–5249.
30 (*a*) M. J. Kamlet, J.-L. Abboud and R. W. Taft, *J. Am. Chem. Soc.*, 1977, **99**, 6027–6038; (*b*) C. Laurence, P. Nicolet, M. T. Dalati, J.-L. M. Abboud and R. Notario, *J. Phys. Chem.*, 1994, **98**, 5807–5816.
31 L. G. S. Brooker, A. C. Craig, D. W. Heseltine, P. W. Jenkins and L. L. Lincoln, *J. Am. Chem. Soc.*, 1965, **87**, 2443–2450.
32 R. E. Dawson, A. Hennig, D. P. Weimann, D. Emery, V. Ravikumar, J. Montenegro, T. Takeuchi, S. Gabutti, M. Mayor, J. Mareda, C. A. Schalley and S. Matile, *Nat. Chem.*, 2010, **2**, 533–538.